# Supporting Information

# Nanopore identification of single nucleotide mutations in circulating tumor DNA by multiplexed ligation

Nitza Burck[1], Tal Gilboa[1,2,3], Abhilash Gadi[4], Michelle Patkin Nehrer[1], Robert J. Schneider[4,#] Amit Meller[1,5,#]

1. Department of Biomedical Engineering, Technion- IIT, Haifa, 32000 Israel
2. Department of Pathology, Brigham and Women's Hospital, Harvard Medical School, Boston, MA 02115
3. Wyss Institute for Biologically Inspired Engineering, Harvard University, Boston, MA 02115
4. Department of Microbiology, NYU School of Medicine, New York, NY 10016, USA
5. Russell Berrie Nanotechnology Institute, Technion- IIT, Haifa Israel.

# co-corresponding authors. Emails: Robert.Schneider@nyumc.org, ameller@technion.ac.il

**Table of Contents:**

## 1. Engineered MB-231 cells

MB-231 cells, highly aggressive, triple-negative breast cancer cell line, were cultured in DMEM with L-glutamine (Corning), 10% FBS, 1% penicillin/ streptomycin (Life Technologies), 1 mM sodium pyruvate (Thermo Scientific) at 37°C and 5% $CO_2$. 15 base pair segments corresponding to different wild type or mutant sequences were linked together and synthesized (IDT) to be used as our assay targets. The synthetic DNA was inserted into a pTRIPZ lentiviral vector by the Gibson assembly using NEBuilder® HiFi DNA Assembly kit (New England Biolabs, #E5520). Once the plasmids were validated by sequencing, pantropic pseudoviral particles containing them were generated. The pTRIPZ vector was packed using Cellecta´s psPAX2/pMD2.G mix for delivery into 293 HEK cells. 48 hours post co-transfection, the lentiviruses were collected and used to infect the MB-231cells. Cells were cultured in DMEM with L-glutamine (Corning), 10% FBS, 1% penicillin/ streptomycin (Life Technologies), 1 mM sodium pyruvate (Thermo Scientific) at 37°C and 5% $CO_2$. Viral transfer occurred 24 hours after seeding in 12-well plates with $2x10^4$ cells/ml. Transduction proceeded for 48 hours, after which cells were trypsinized and moved to a 10 cm dish. Puromycin antibiotic (4 ug/mL) ensured effective positive selection of transfected cells. To further ensure plasmid incorporation, TurboRFP was induced in the transduced cells using Doxycycline.

## 2. Development of xenotransplant tumors, isolation of cfDNA

Approximately $5x10^6$ of the newly engineered MB-231 cell line (either unmutated or mutated) were injected into the flank of nude mice under anesthetic effect of Isoflurane. Typically, tumors arise within two weeks and begin to metastasize within a month. At 5-6 weeks mice were anesthetized with isoflurane, exsanguinated by aortic cardiac puncture, collecting on average 1.5 ml of blood per mouse. For cfDNA isolation, blood sera was prepared from fresh blood specimens by centrifugation, sera removed, particulate matter removed from sera by a second centrifugation, then DNA isolated using the Invitrogen MagMax cfDNA isolation kit, a magnetic bead approach developed for a highly efficient purification of small amounts of short (<300 bp) DNA fragments that exclude large DNAs. Quantification of cfDNA was carried out by Nanodrop analysis showing about 100ng of DNA were collected from each group of mice.

## 3. Probe design for mutation identification

| Mutation | Signal probe | Separation probe |
|---|---|---|
| ERBB2 S310F | /5AmMC6/TTTTTTTTTTTTTTTTTTT/iAmMC6T/ TTTTTTTTTTTTTTTTTT/iAmMC6T/GTCATAGCGGGTCCCTC | /5Phos/GACACTTTGGGTGCAGAATCC/3Bio |
| PIK3Ca H1047R | /5AmMC6/TTTTTTTTTTTTTTTTTTT/iAmMC6T/ TTTTTTTTTTTTTTTTTTT/iAmMC6T/ATGACGTGCATCATCTGCT | /5Phos/TA GTG ATT TCC TGA TCA GGA TCC G/3Bio/ |

**Table S1.** Sequences of Detection probe sets designed to detect ERBB2 S310F and PIK3Ca H1047R mutations.

## 4. Ligation reaction optimization and yield calculation

Ligation conditions were optimized, including the buffer, ligation cycle number and ratio of probes to template.

### 4.1. Buffer and number of cycles optimization:

Four buffers were compared for ligation efficiency, including commercial NEB buffer and three in-house prepared buffers.

| | **NEB buffer** | **Buffer 0** | **Buffer 1** | **Buffer 2** |
|---|---|---|---|---|
| Tris-HCl | 20mM | 20mM | 20mM | 20mM |
| Potassium Acetate | 25mM | 100mM | 200mM | 100mM |
| Magnesium Acetate | 10mM | 2.5mM | 2.5mM | 1mM |
| NAD 1 | 1mM | 1mM | 1mM | 1mM |
| DTT | 10mM | 10mM | 10mM | 10mM |
| Triton® X-100 | 0.1% | 0.1% | 0.1% | 0.1% |
| pH | 7.6 | 7.6 | 7.6 | 7.6 |

**Table S2.** Buffer components for ligation buffer optimization

Each buffer was tested with 10, 20 and 40 ligation cycles. The samples were run on a 20% PAGE denaturing gel (Figure S1). Each ligation band was quantified in comparison to the DNA template to assess the ligation yield (Figure S2). Buffer 2 was the most effective at high cycle numbers, however the commercial NEB buffer achieved high ligation efficiency at low cycle numbers. Buffer 2 was used for all shown experiments.

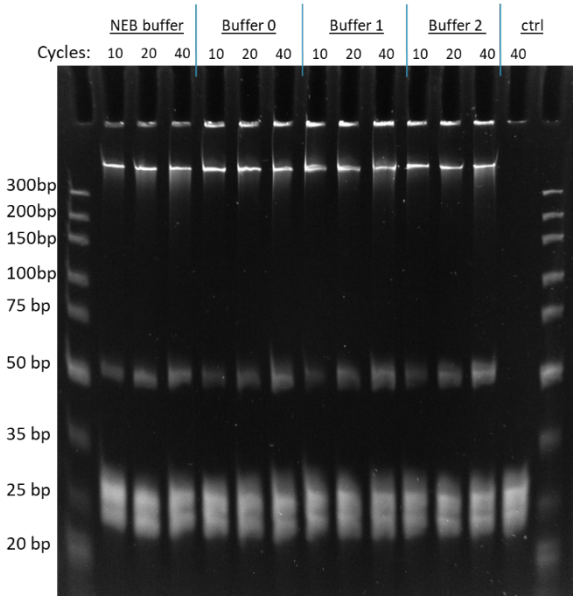


**Figure S1.** Buffer Optimization.
20% Denaturing PAGE of buffer optimization. Four different buffers were tested for 3 amounts of cycles for the same probe combination. The negative control does not contain bacterial template DNA.

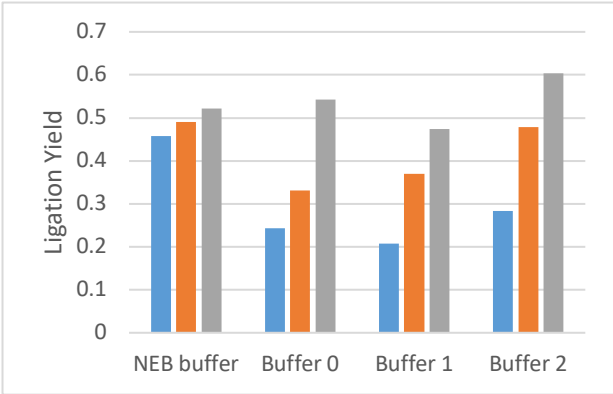


**Figure S2.** Quantification of buffer optimization gel (Figure S1) assessing ligation with four buffer compositions for varying numbers of ligation cycles: 10 cycles (blue), 20 cycles (orange), 40 cycles (gray).Each ligation band was quantified and normalized against the number of template molecules to calculate the reaction yield.

**4.2. Ratio of template to probes optimization:**

The optimal concentration ratio between template DNA and ligation probes was explored. The template DNA amount was kept constant at 100ng in each reaction. The number of probes added was varied at values of 10X, 100X, 250X and 500X the template amount. A steady increase in ligation efficiency was observed as a larger number of probes were added (Figure S3). The 1:100 ratio was sufficient to observe a DNP, but 1:500 exhibited a significant increase. However, for cost-benefit analysis purposes we chose to proceed with the 1:100 ratio for proof-of-concept experiments, to save the cost of ligation probes.

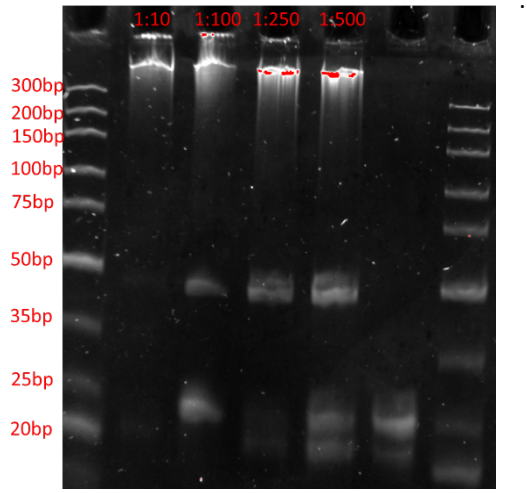


**Figure S3.** Optimization of Ligation Probe Ratio. The optimal concentration ratio between template to probes for the ligation detection reaction was analyzed (1:10, 1:100, 1:250 and 1:500) on a 20% denaturing PAGE gel.

### 4.3. Yield calculation for ligation reaction for the detection of ERBB2 S310F and PIK3Ca H1047R mutations

Using the optimal conditions we found (100 ng template, 1:100 templates:probes ratio, 30 heating cycles in buffer #2) we performed the ligation reaction using our plasmid template and designated probes (table S1). The ligation reaction was carried out as described in the methods section. The reaction mixed was then analyzed on a 20% denaturing PAGE gel (Figure S4). Comparing the intensity of the free probes vs. the ligation product and using the number of cycles and known ratio of templates to probe we calculated the reaction yield. For the ERBB2 S310F mutation we had a total average of 20.71 product molecules per template, or a yield of 72.19% per cycle. For the PIK3Ca H1047R mutation we had a total average of 15.78 product molecules per template, or a yield of 55% per cycle.

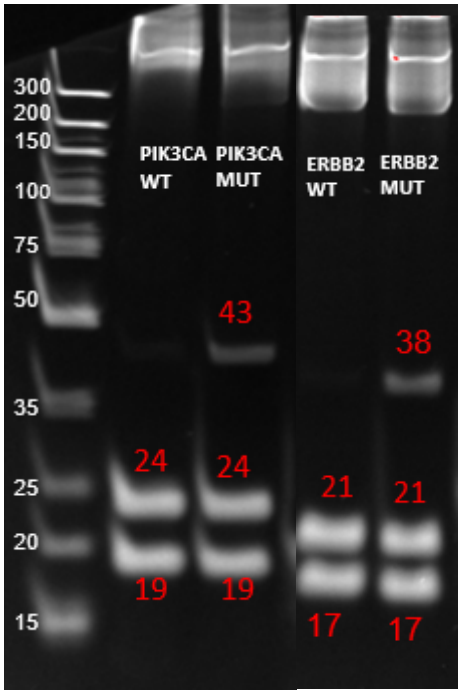


**Figure S4.** Ligation reaction detecting the presence of ERBB2 S310F and PIK3Ca H1047R mutations on a 20% denaturing PAGE gel.

## 5. Probe labelling efficiency validation

The ERBB2 S310F signal probe was labelled with an optical barcode of 3 DyLight650 dyes. The PIK3Ca H1047R signal probe was labelled with an optical barcode of 3 DyLight550 dyes. Conjugation was confirmed by UV-vis absorption spectroscopy (Agilent Technologies cary60 UV-Vis) as shown in Figure S1 panels a and c. In order to account for free dyes that remained in the solution even after beads separation and ethanol precipitation, the probes were subjected to a quick (10 minutes) gel electrophoresis (20% PAGE) as shown in figure S1 panels b and d. The gel images were processed using Image-J gel processing software package determining the ratio of conjugated to free dyes in the solution according to band intensity. Finally, we calculated the labelling efficiency and found thar that the ERBBE probe was averagely labelled with 2.5 dyes, while the PIK3Ca probe had an average of 2.84 labels.

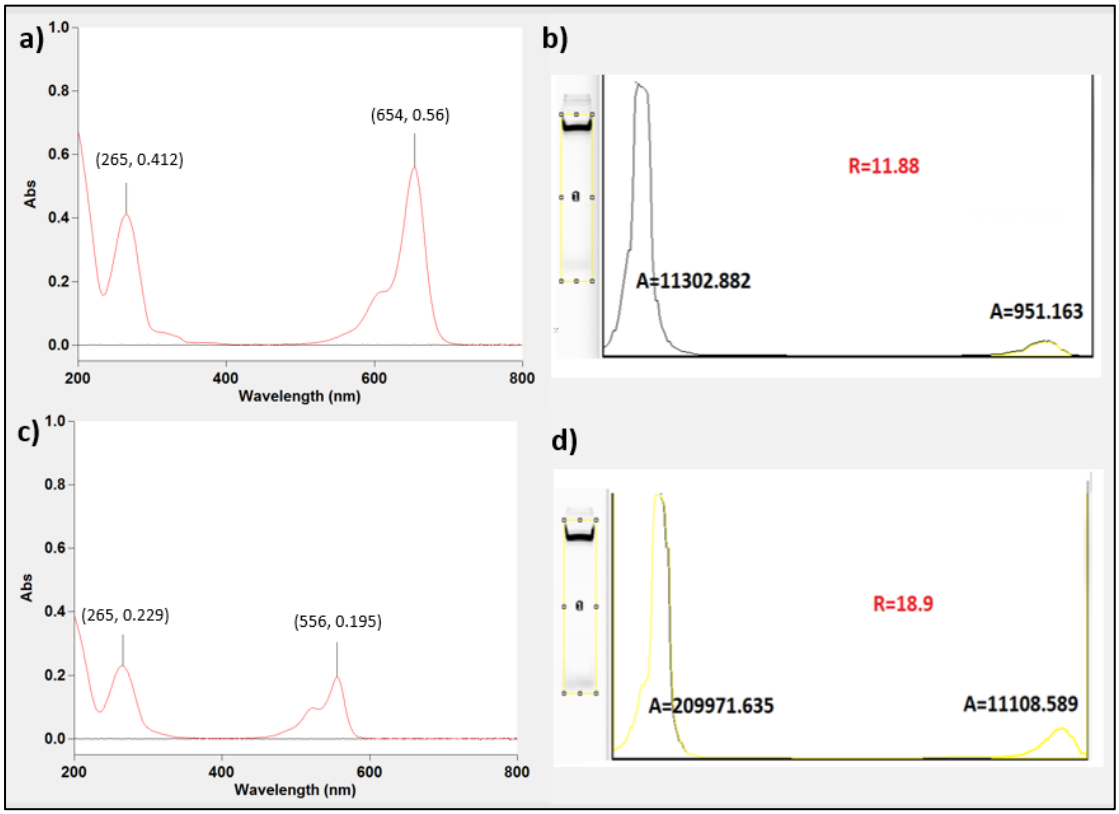


**Fig S5.** Confirmation of dye conjugation to the detection probes. UV-VIS absorption spectra show the ratio between DNA and dye concentrations for: (a) ERBB2 probe, and for the (c) PIK3Ca mutation. PAGE analysis was then used to accounts for free dyes in the solution. PAGE analysis of free dyes and image processing results are shown on the top right for ERBB2 (b) and on the top bottom for PIK3Ca (d).

## 6. Streptavidin coated beads separation

Following ligation, streptavidin-coated magnetic beads (Dynabeads MyOne Streptavidin C1) were used to capture the short biotinylated probe and the longer labelled newly formed ligation product. In this process we also wash away the remainder of the sample, free dyes that are left and the unligated labelled probes. 20µl of the magnetic beads were re-suspended in 100 µl of "Binding and washing buffer" (B&W) (50 mM Tris-HCl (pH 7.5), 0.5mM EDTA, 1M NaCl, 0.1% Tween). This washing step was repeated two more times. After the final wash step, the beads were re-suspended in 2x B&W and the ligation product was added such that the final concentration of NaCl is 1M. The sample was then left gently rotating for 30 minutes at room temperature to allow the biotinylated DNA to bind to the streptavidin coated beads. The beads were then held with a magnet and the solution was removed. The beads were then washed three times with 100 µl of B&W buffer to wash away any DNA that had not bound to the beads. Followed by a wash with 100 µl dd$H_2O$ and then 50 µl of 0.15 M NaOH for 10 minutes in order to denature any strands bound the immobilized DNA. After being placed on the magnet again, the beads are resuspended in 20 µl DDW eluted by heating the sample to 95 ˚C for 30 minutes. This process breaks the biotin-streptavidin bond and using a magnet to hold the beads, the ligation product sample can be recovered.

## 7. Nanochip fabrication for electro-optical sensing

Wafer-scale fabrication of $TiO_2$ nanopore chip

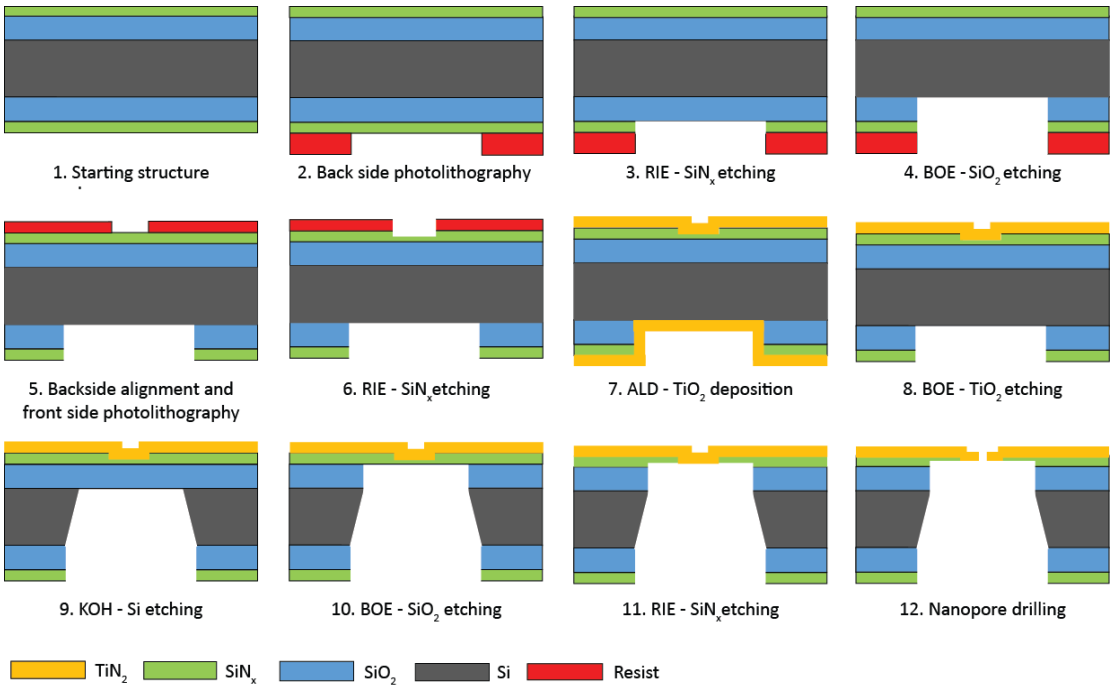

**Figure S6.** A Stepwise schematic description of a wafer scale $TiO_2$ nanopore sensor fabrication.[1] The fabrication started with a 360 µm thick, 4'' diameter and crystal orientation Si wafer coated with 500 nm SiO2 and 50 nm silicon nitride on both sides. $SiN_x$ was deposited using Low Pressure Chemical Vapor Deposition (LPCVD). The fabrication process can be divided into four main steps:

(1) *Preparation (steps 1-4).* The wafer was cleaned thoroughly using acetone, methanol and isopropanol, then rinsed with DI water and spun dry (step 1). The back side of the wafer was coated with AZ1518 resist (step 2) at 5000 rpm for 1 min and baked at 110$^o$ C for 2 min on a hot plate. Square patterns and dice lines were patterned using direct-write photolithography (MicroWriter ML3, DMO). The $SiN_x$ and $SiO_2$ were etched using $CF4/O_2$ reactive ion etch (RIE, Diener Electronic) and controlled buffered oxide etch (BOE), respectively (steps 3 and 4) creating a hard mask.

(2) *Thin region fabrication (steps 5 -7).* The front side of the wafer was spin-coated with AZ1518 resist. Backside alignment was used to align thin regions on the front side to the square patterns on the back side. The thin regions with diameter of 2 µm were patterned using direct-write photolithography as shown in step 5. The exposed SiNx was thinned down to ~10 nm with RIE. The wafer was then cleaned by acetone, isopropanol and DI water to remove the resist (step 6) and was immediately treated with UV/Ozone prior to being put into the atomic-layer deposition (ALD, Arradiance GEMStar XT) chamber. 15 nm thick TiO2 was deposited on both sides using ALD (step 7). TDMAT and water were used as a precursor and an oxidizer, respectively, yielding a growth rate of 0.43 Å/cycle at 200$^o$ C.

(3) *Fabrication of the free-standing membrane (steps 8-11)*. The $TiO_2$ layer on the back side was first etched by BOE (step 8). The exposed Si was anisotropically etched by KOH solution (step 9). The KOH was stopped immediately when the Si was completely etched in order to avoid penetration to the front side. Finally, the second $SiO_2$ layer was etched by BOE, resulting in a free-standing $TiO_2/SiN_x$ membrane (step 10). To fabricate a free-standing $TiO_2$ membrane in the thin region surrounded by a $TiO_2/SiN_x$ bilayer, $SiN_x$ was etched from the bottom side by calibrated RIE, which has a negligible etching rate for $TiO_2$ (step 11).

(4) *Fabrication of $TiO_2$ nanopore (step 12).* The nanopores were drilled in the thin regions using either Controlled Dielectric Breakdown (CDB). For this end we used the voltage-pulsed strategy as described before.[2] Pulses of 8V (60 ms long) were applied on the membrane. Current jump, indicating of pore formation, was observed in less than 10 minutes.

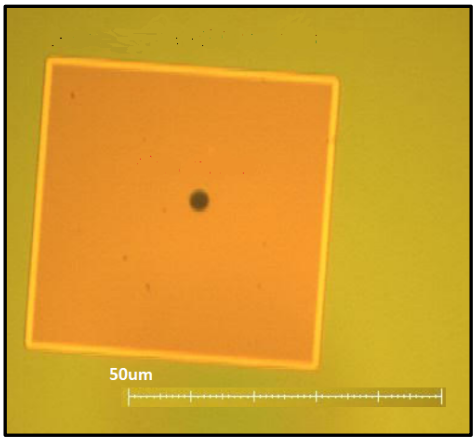


**Fig S7.** TiO2 chip examined under a bright field microscope with a 100X objective. The membrane (47 µm x 47 µm) can be observed, as well as the presence and location of the thinner region (2.3 µm diameter) where the pore is formed.

**8. Nanopore fabrication**

Prior to drilling, chips were pre-treated by washes of organic solvents (Acetone, Methanol and Isopropanol) and then treated with UV/Ozone for 5 minutes on each side. Chips were then glued with PDMS to custom-designed inserts, which will later fit on the electro-optical set-up. Fabrication of a nano-scale pore in the $TiO_2$ thin region was performed using Controlled Dielectric Breakdown (CDB).(31,34) A voltage is applied across the insulating membrane generating a high electric field in it. The process is performed in aqueous solution of 1M KCl, which the chip will remain in throughout the experimental process. Ag/AgCl electrodes immersed on both sides of the membrane are connected to a current amplifier. The induced leakage current is monitored in real-time by a custom LabView program, so that when the current exceeds a pre-set threshold (typically 2 nA current), voltage bias is ceased immediately. This is done in combination with a voltage-pulsed strategy, optimizing the probability only one highly size-controlled pore is drilled in the membrane. For a 20 nm thick TiO2 layer, pulses of 8V, 60 ms long were used to drill pores with a diameter of ~2 nm (1.8-3 nA current @ 300mV).

## 9. The electro-optical experimental setup

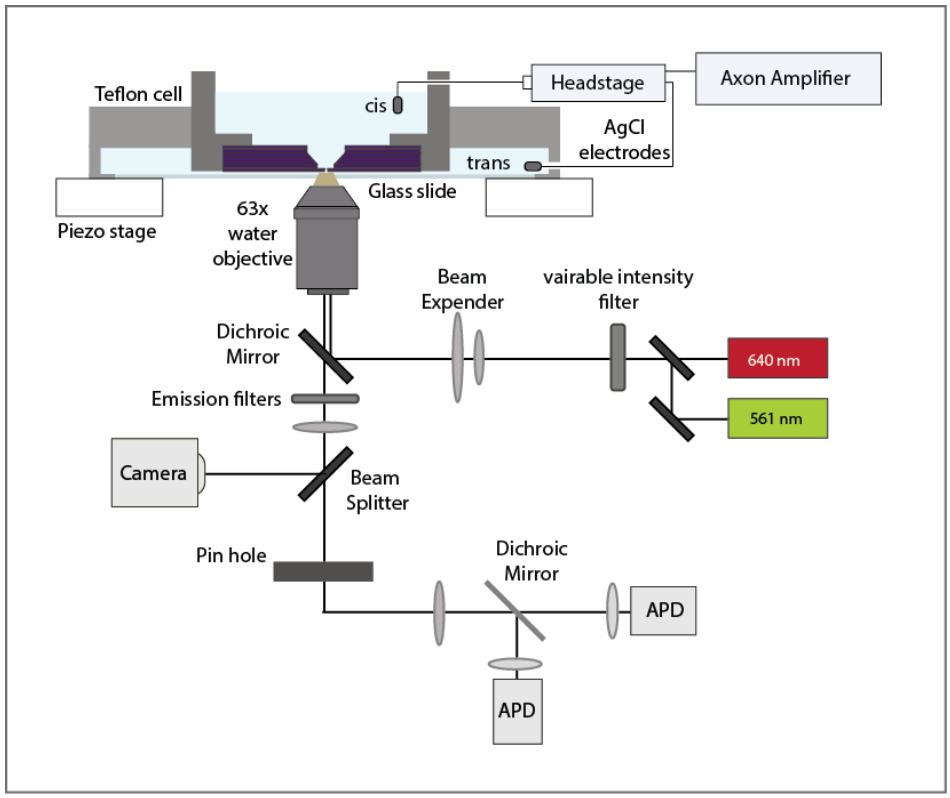


**Fig S8.** A schematic diagram of the electro-optical setup used for single-molecule mutation readout. Two colored laser-excitation at 561 nm and 640 nm are used to create a confocal illumination spot at the pore to excite the fluorescent labels of the molecules as they pass through the pore. The emitted photons are collected using a high numerical aperture (NA) objective, spatially filtered using a pinhole, and a dichroic mirror is used to spectrally split the light which is monitored using two Single-Photon counting Avalanche Photo-Diode sensors (SPAPDs). A small fraction of the reflected laser is continuously monitored using a camera to preserve the laser focusing. Abbreviations: LP, Long Pass; APD, Avalanche Photodiode.

## 10. Data acquisitions and analysis of electro-optical events

### Data acquisition

During an experiment a custom LabVIEW (LV) program detects electrical translocation events according to threshold parameters set by the user. These events, in addition to a specific padding of typically 30 ms before and after each event, are concatenated and saved. The optical signals detected at the same period by each APD (see Experimental setup) are

concatenated and saved as well. To synchronize the electrical and optical data acquisition, the two cards were triggered and synchronized via a common hardware connection. In addition to the raw data we save a text file containing information about the experiment and a list with the start index and end index of each event. This data is used to extract the events from the binary data files for offline analysis.

**Data analysis**

The offline analysis for each event starts by extracting the dwell time ($t_D$), and the amplitude drop ($IB=I_{blocked}/I_{open}$), of its electrical signal according to the electrical threshold. Then a second sequential analysis is performed on the same padded event according to the optical threshold to obtain the start time of the optical signal ($t_{start\_opt}$), the end time ($t_{end\_opt}$) and the total dwell time of the optical signal ($t_O$). The optical data between $t_{start\_opt}$ and $t_{end\_opt}$ is extracted and integrated to obtain the number of photons emitted during the entire optical event (Figure S4). Finally the average photon flux during the optical event (sum of the number of counts during the optical event divided by $t_O$), and the photon fluxes before and after each of the optical events (representing the optical background for each event), are calculated.[3]

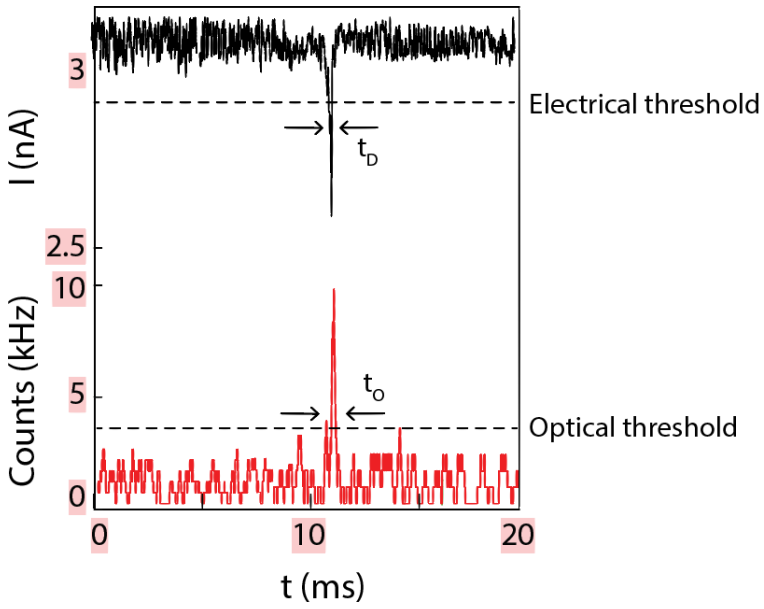


**Figure S9.** Event analysis. For each event the electrical signal is analyzed according to an electrical threshold (upper dashed line) to extract the dwell time of the electric event ($t_D$). Then the optical signal is analyzed according to an optical threshold (lower dashed line) to extract the dwell time of the optic event ($t_O$).

## 11. Electrical translocation events of cfDNA from mice blood

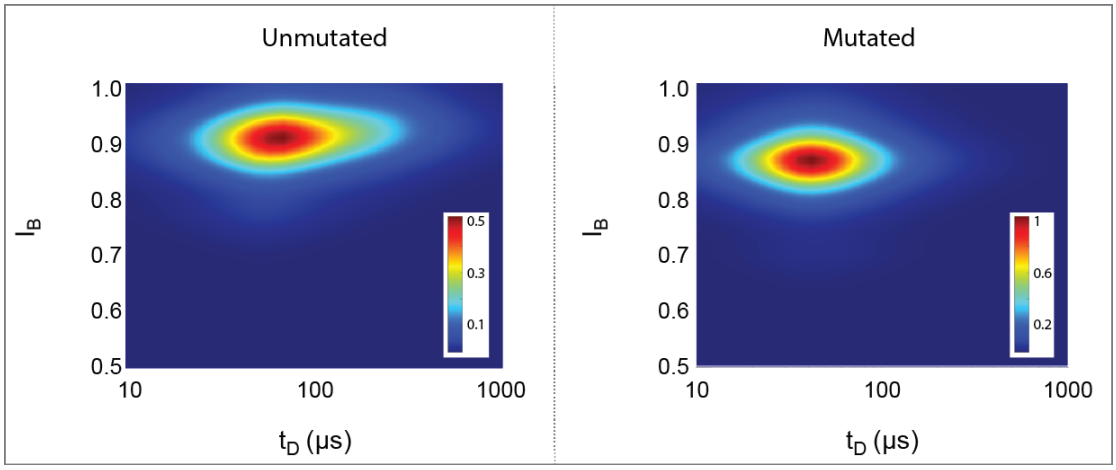


**Figure S10.** Single-molecule nanopore analysis of the mutated and unmutated cfDNA directly from mice blood. Electrical scatter plot of the blocked current ($I_B$) versus dwell time ($t_D$) shows that both samples are detected electrically in the nanopore device.

## 12. Specificity estimation

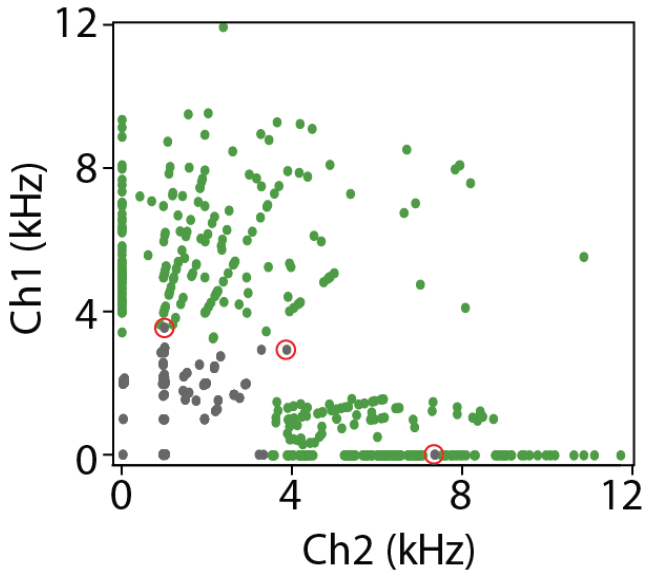


**Figure S11.** Scatter plot of the mutated (green) and unmutated (grey) optical events. The optical threshold was used to classify the unmutated cfDNA and evaluate the specificity. The three false negatives are marked with red circles.

## 13. References:


1. Wang R, Gilboa T, Song J, Huttner D, Grinstaff, MW, Meller A. Single-molecule discrimination of labeled DNAs and polypeptides using photoluminescent-free $TiO_2$ nanopores. ACS Nano 2018; 12: 11648–56.

2. Zrehen A, Gilboa T, Meller A. Real-time visualization and sub-diffraction limit localization of nanometer-scale pore formation by dielectric breakdown. Nanoscale 2017; 9: 16437–45.

3. Gilboa T, Torfstein C, Juhasz M, Grunwald A, Ebenstein Y, Weinhold E, Meller A. Single-molecule DNA methylation quantification using electro-optical sensing in solid-state nanopores. ACS Nano 2016; 10:8861–70.